DOI: 10.1002/ejic.201001103

Relaxometric Study of a Series of Monoaqua Gd^{III} Complexes of Rigidified EGTA-Like Chelators and Their Noncovalent Interaction with Human Serum Albumin

Mauro Botta,*[a] Stefano Avedano,[a] Giovanni Battista Giovenzana,[b] Alberto Lombardi,[b] Dario Longo,[c] Claudio Cassino,[a] Lorenzo Tei,[a] and Silvio Aime*[c]

Keywords: Lanthanides / NMR spectroscopy / Imaging agents / Relaxometry

The lanthanide(III) complexes of five EGTA [ethyleneglycol-bis(2-aminoethyl) ether-*N*,*N*,*N*′,*N*′-tetraacetic acid] derivatives fused with aromatic (benzene: **L1**; naphthalene: **L2**) and functionalized aromatic (**L3**–**L5**) moieties on the oxyethylene bridge were investigated in aqueous solution. ^{1}H and ^{13}C NMR spectra of the La^{III} and Lu^{III} complexes of **L1** and **L2** indicate that the structural differences across the Ln series found for the $[Ln(EGTA)]^{-}$ complexes is maintained in the new derivatives. The presence of the aromatic moiety favours an increased stereochemical rigidity, as assessed by VT ^{13}C NMR spectra. Temperature-dependent ^{17}O NMR spectroscopic data and $1/T_1$ ^{1}H NMRD profiles of the Gd^{III} complexes of **L1**–**L3** were measured and globally analyzed to obtain the parameters influencing the water exchange rate, k_{ex}, and rotational dynamics. The k_{ex} values are ca. twice as high as the corresponding value of $[Gd(EGTA)]^{-}$ and very close to optimal. The lipophilic complexes $[Gd\mathbf{L4}]^{-}$ and $[Gd\mathbf{L5}]^{-}$ form micellar aggregates whose NMRD profiles were measured and analyzed in terms of a model that allows separation of global motion and local rotation. The noncovalent binding interaction of the complexes to human serum albumin and the relaxivity of the macromolecular conjugates were investigated with relaxometric techniques at 20 MHz and 298 K, and the importance of a restricted local motion of the complex at the binding site for attaining large relaxivity enhancement outlined. Theoretical docking simulations and relaxometric competition experiments provided insights into the binding modes of the complexes.

Introduction

A series of five acyclic polyaminopolycarboxylate ligands (**L1**–**L5**; Scheme 1) derived from the basic structure of EGTA [ethyleneglycol-bis(2-aminoethyl) ether-*N*,*N*,*N*′,*N*′-tetraacetic acid] with the incorporation of an aromatic group into the oxyethylene bridge has been recently synthesized in order to maintain or even improve the structural and relaxometric properties of the corresponding Gd^{III} complexes.[1] As shown some 10 years ago,[2] the water exchange rate for the $[Gd(EGTA)(H_2O)]^{-}$ [H_4EGTA = ethyleneglycol-bis(2-aminoethyl) ether-*N*,*N*,*N*′,*N*′-tetraacetic acid] complex is $3.1 \times 10^7\ s^{-1}$ (298 K), and this value is one order of magnitude higher than that typical of the clinically used MRI probes $[Gd(DOTA)(H_2O)]^{-}$ (H_4DOTA = 1,4,7,10-tetraazacyclododecane-*N*,*N*′,*N*′′,*N*′′′-tetraacetic acid) and $[Gd(DTPA)(H_2O)]^{2-}$ (H_5DTPA = diethylenetriamine-*N*,*N*′,*N*′′-pentaacetic acid) and one of the fastest reported for nine-coordinate polyaminopolycarboxylate Gd^{III} complexes.[2,3] In spite of this favourable property, explained by the steric compression at the water binding site exercised by the oxyethylene bridge present in the tricapped trigonal-prismatic structure, no further studies have been reported regarding the preparation of macromolecular derivatives of high relaxivity.

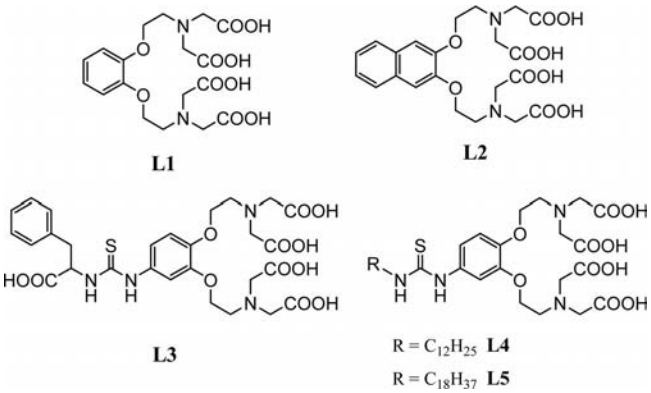

Scheme 1. Ligands discussed in this work.

[a] Dipartimento di Scienze dell'Ambiente e della Vita, University of Piemonte Orientale "Amedeo Avogadro",
Viale Teresa Michel 11, 15121 Alessandria, Italy
Fax: +39-0131-360250
E-mail: mauro.botta@mfn.unipmn.it
[b] DiSCAFF & DFB Center, University of Piemonte Orientale "Amedeo Avogadro",
Via Bovio 6, 28100 Novara, Italy
[c] Center for Molecular Imaging, Department of Chemistry IFM, University of Turin,
Via Nizza 52, 10126 Torino, Italy
E-mail: silvio.aime@unito.it

Supporting information for this article is available on the WWW under http://dx.doi.org/10.1002/ejic.201001103.

The five novel EGTA-like chelators are potentially octadentate and are expected to retain the favourable complexing properties of the parent ligand towards lanthanide(III) cations. In a previous study, it has been reported that, whereas the chemical modification on the basic ligand backbone appears to impact the thermodynamic stability of the complexes with Ca^{II}, Mg^{II}, Cu^{II} and Zn^{II}, the $\log K$ values of some of the novel ligands with La^{III}, Gd^{III} and Lu^{III} differ only slightly from the values of the corresponding EGTA complexes.[1] In addition, the aromatic moiety and the hydrophobic substituents allow the complexes either to interact noncovalently with HSA or to aggregate into micellar systems. In a recent communication, we have shown that the combination of a reduced internal mobility with a high rate of water exchange results in a remarkable increase in the relaxivity of the [Gd**L2**]$^{-}$–HSA adduct, up to a value of 80 $mM^{-1}s^{-1}$, quite similar to that predicted by theory (100–120 $mM^{-1}s^{-1}$) and unprecedented to the best of our knowledge for such systems.[4]

In this work, we report on the solution structures and dynamics of the diamagnetic La^{III} and Lu^{III} complexes obtained from ^{1}H and ^{13}C NMR spectroscopy. A detailed characterization of the Gd^{III} complexes with **L1**–**L5** and of their binding affinity to HSA was performed in aqueous solution by relaxometric techniques. To this purpose, we have investigated the ^{1}H relaxivity dependence on pH, temperature, magnetic field strength and protein concentration. Information on the water exchange dynamics has been obtained from temperature-dependent ^{17}O NMR spectroscopic data. Finally, insight into the nature of the interaction of the complexes with the protein has been gained through combined modelling and PRE (proton relaxation enhancement)[5] studies.

Results and Discussion

Solution Structures

The proton and carbon NMR spectra of the diamagnetic complexes [Ln**L1**]$^{-}$ and [Ln**L2**]$^{-}$ (Ln = La and Lu), measured in D_2O at neutral pH over the temperature range 273 to 353 K, correspond rather closely to those observed for the [Ln(EGTA)]$^{-}$ complexes.[2] In this latter case, two coordination polyhedra are adopted by the ligands for the early and late members of the lanthanide series with a break around Nd–Sm. The complexes with the lighter lanthanides adopt a bicapped square-antiprismatic coordination geometry where the capping positions are identified by the two nitrogen atoms. Each of the two square faces, connected by the ethylenedioxy bridge, is formed by one of the ether oxygen atoms, two oxygen atoms of adjacent carboxylate groups and one water molecule. Because of a fast fluxional process, only a small number of resonances are detected in both the ^{1}H and the ^{13}C NMR spectra of the diamagnetic La^{III} chelate. A strictly similar behaviour is observed for [La**L1**]$^{-}$ (Figure 1) and [La**L2**]$^{-}$ (Figures S1, S2). The proton spectrum of [La**L1**]$^{-}$ shows a relatively broad peak (δ = 6.83 ppm) corresponding to the aromatic protons, two singlets for the methylene protons of the ethylene groups (δ = 2.80 and 4.05 ppm) and one AB spin system for the eight acetate protons (3.15 and 3.20 ppm; ^{2}J = 16.5 Hz). A pronounced degree of nonstereochemical rigidity characterizes this complex and results in an average of the NMR peaks of pairs of atoms in aqueous media even at low temperatures. The fluxional process is likely to involve a rotation of the two square faces of the coordination polyhedron around the C–C bond of the oxyethylene bridge with a concerted

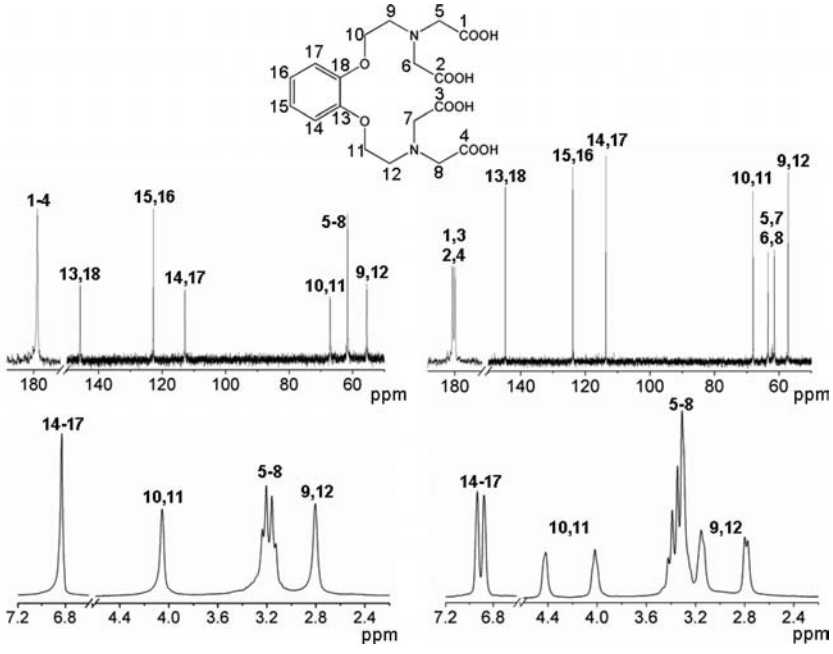

Figure 1. ^{1}H (bottom) and ^{13}C (top) NMR spectra of the La^{III} (left) and Lu^{III} (right) complexes of **L1** at 11.7 T and 278 K.

conformational inversion of the ethylene moieties. In agreement with this hypothesis, the four carbonyl carbon atoms and the four methylene carbon atoms of the acetate arms generate a single peak in the corresponding ^{13}C NMR spectrum at 278 K.

In the case of the EGTA complexes with the heavier lanthanides (Sm–Lu), the cation is nine-coordinate and features one water molecule in its inner coordination sphere. The coordination polyhedron is best described as a tricapped trigonal prism, in which the capping positions are occupied by the two nitrogen atoms and the inner sphere water oxygen atom, and the trigonal faces are formed by the ether oxygen atoms and the carboxylate groups. The ^{13}C NMR spectrum of [Lu**L1**]$^-$ is consistent with this solution structure, as a pair of distinct signals is recorded for the carbonyl and the methylene carbon atoms of the acetate arms. Accordingly, in the proton spectrum, a doubling of the peaks of the aliphatic protons is observed (Figure 1). These spectroscopic data are consistent with a rapid scrambling process of two carboxylate groups situated on adjacent vertices of the two trigonal planes. As the temperature is increased, a general reduction and sharpening of the resonances suggest that a further dynamic rearrangement is taking place on the NMR timescale. Evaluation of the process is better tackled on the basis of the variable-temperature (VT) ^{13}C NMR spectra (see Supporting Information), in particular by looking at the region of the acetate absorption bands. As the temperature is increased the two methylene peaks at δ = 61.7 and 63.6 ppm broaden, coalesce (T = 319 K) and then merge into a single resonance at δ = 62.9 ppm. From the chemical shift difference of the two peaks in the low-temperature limiting spectrum and the coalescence temperature, we may estimate the free energy of activation for this dynamic process to be $\Delta G^{\#}$ = 62.0 kJ mol^{-1}.[6] Analogously, for [Lu**L2**]$^-$, a $\Delta G^{\#}$ value of 63.8 kJ mol^{-1} can be calculated. A strictly similar behaviour is observed in the correlated carbonyl region. The corresponding process for [Y(EGTA)]$^-$ has been reported to be characterized by a $\Delta G^{\#}$ value of 58.0 kJ mol^{-1}.[7]

In summary, the incorporation of a rigid aromatic group in the ligand backbone has only a marginal effect on the solution structure and dynamics of the complexes, in line with the small changes observed for their thermodynamic stability constants. The most relevant consequence of the chemical modification is the pronounced increase in the stereochemical rigidity that could affect the relaxometric properties of the corresponding Gd^{III} derivatives.

Relaxometric Properties

The relaxivity of the Gd^{III} complexes with **L1**–**L5** has been measured at 20 MHz and at 298 K (Table 1). The values are aligned with the data for monoaqua low molecular weight gadolinium(III) chelates, which indicates that all the EGTA derivatives retain the same hydration number (q = 1) and the nine-coordinate ground state of the parent [Gd(EGTA)]$^-$ complex.[8,9] The r_{1p} values increase linearly with molecular weight from [Gd(EGTA)]$^-$ to [Gd**L4**]$^-$ (in the nonaggregated form before the critical micellar concentration, see below), whereas for [Gd**L5**]$^-$, the relaxivity is sensibly higher and indicates the formation of larger aggregates (Figure 2). The behaviour of r_{1p} with pH, measured for [Gd**L1**]$^-$ and [Gd**L5**]$^-$ follows strictly that reported for [Gd(EGTA)]$^-$: the relaxivity assumes a constant value in the interval 4–11 and it increases sharply at more acidic pHs, following partial dissociation of the complex and progressive release of the metal ion. These complexes are then stable over a broad pH range with respect to hydrolysis, hydration and coordination equilibria. The NMRD (nuclear magnetic relaxation dispersion)[10] profiles were measured at 298 K over the proton Larmor frequency range 0.01–70 MHz (Figure 3). The profiles of the [Gd**L1**–**L4**]$^-$ complexes are characterized by a simple shape featuring a single dispersion centred around 4–8 MHz, quite typical of rapidly tumbling q = 1 complexes.[11,12]

Table 1. Selected best-fit parameters derived from the global analysis of ^1H NMRD profiles (298 K) and ^{17}O NMR spectroscopic data (2.1 T) for Gd^{III} complexes.

	EGTA[a]	**L1**	**L2**[b]	**L3**[b]	**L4**[c]
$^{298}r_{1p}$ [mM^{-1} s^{-1}]	4.7	5.1	6.0	7.0	7.6
τ_M [ns]	32	12	18	10	[d]
τ_R [ps]	58	68	100	122	140
τ_V [ps]	24	23	24	24	29
Δ^2 [10^{19} s^{-2}]	3.4	4.5	4.5	4.5	2.9
$\Delta H_M^{\#}$ [kJ mol^{-1}]	42.7	14.0	13.8	10.0	/
$\Delta S_M^{\#}$ [J mol^{-1} K^{-1}]	+42	–46	–50	–59	/
r [Å][e]	3.1	3.0	3.0	3.0	3.0
q[e]	1	1	1	1	1
$A/\hbar$ (10^6 rad s^{-1})	–3.2	–3.5	–3.5	–3.6	–

[a] Ref.[2] [b] New analysis of data in ref.[4] [c] Before the critical micellar concentration. [d] This value was fixed to 15 ns during the fit of the NMRD data. [e] Fixed in the fitting procedure.

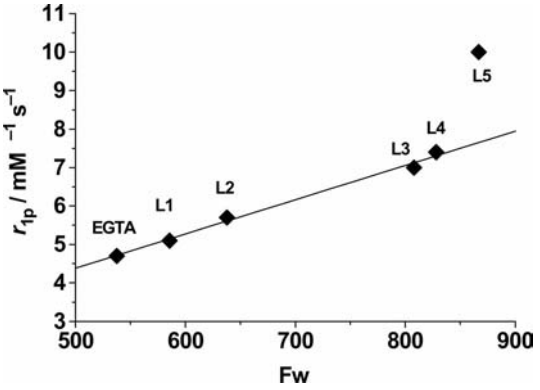

Figure 2. Proton relaxivities (20 MHz, 298 K) as function of molecular weight for the [Gd**L1**–**L5**]$^-$ complexes.

The small differences in the inflection point and amplitude among the NMRD profiles are simply explained on the basis of the differences in the molecular weight of the complexes that affect the reorientational correlation time τ_R. The ratio between the r_{1p} values at 0.01 and 60 MHz varies only from 1.51 to 1.76 to suggest similar values of

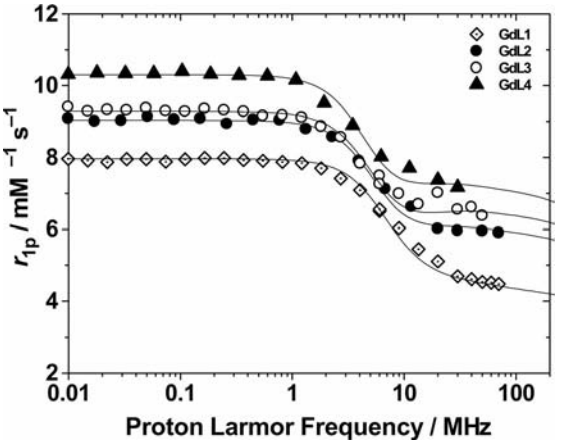

Figure 3. $1/T_1$ ^{1}H NMRD relaxation data for the complexes [Gd**L1**–**L4**]$^-$ at 298 K and pH = 7.2. The concentrations of the aqueous solutions are: 1.5 mM for [Gd**L1**–**L3**]$^-$ and 0.06 mM for [Gd**L4**]$^-$. The solid lines represent the best results of the fitting to the experimental points (see Table 1).

the electronic relaxation times, $T_{1,2e}$. Clearly, the nature of the chemical groups on the aromatic ring of the ligands does not have an appreciable impact on the relaxometric properties of the metal complexes since it only appears to influence their rotational dynamics. This might be a consequence of the poor coordinating ability of the ether oxygen atoms that do not efficiently transmit the electronic effects of the substituents on the periphery of the ligand to the metal ion.

The ^{17}O NMR R_2 values were measured at 2.1 T in the temperature range 5–70 °C for the [Gd**L1**–**L3**]$^-$ complexes (Figure 4).[13] The experimental data show a nearly exponential increase with decreasing temperature, as previously observed for [Gd(EGTA)]$^-$, which indicates the occurrence of a fast exchange regime for the coordinated water molecule. The ^{17}O NMR spectroscopic data were analyzed in terms of the Swift–Connick equations,[14] whereas the NMRD profiles were fitted to the standard equations for the inner- (IS) and outer-sphere (OS) relaxation contributions. The number of parameters is rather large and it is therefore customary to fix some of them to reasonable or typical values:[2,8,9] q = 1, the Gd inner sphere water proton distance r = 3.0 Å, the Gd outer sphere water proton distance a = 4.0 Å, the diffusion coefficient D = 2.24 × 10^{-5} cm^2 s^{-1}, the activation energy of the correlation time for the modulation of the transient zero-field-splitting (ZFS) tensor E_V = 1.5 kJ mol^{-1} and the activation energy of the rotational correlation time E_R = 18 kJ mol^{-1}. In the global fitting procedure, the variable parameters are: the trace of the square of the transient ZFS tensor Δ^2, the correlation time describing its modulation τ_V, the rotational correlation time τ_R, the mean residence lifetime of the inner sphere water molecule τ_M, its enthalpy and entropy of activation ΔH_M and ΔS_M, the scalar Gd–^{17}O$_w$ coupling constant $A/\hbar$. In addition, we used as starting values in the least-square procedure the best-fit values obtained for [Gd(EGTA)]$^-$. For all three novel complexes, the rate of water exchange is higher than for the parent EGTA complex by a factor of 2–3. This may be rationalized by a higher steric crowding of the aromatic moiety relative to the ethylene group, which is not so large to favour the eight-coordinate ground state (q = 0) but pronounced enough to induce a further destabilization of the bound water molecule and thus a decrease in its mean lifetime. In fact, the low values of the enthalpy of activation, $\Delta H_M^{\#}$, and the negative values of the entropy of activation, $\Delta S_M^{\#}$, suggest a dissociative interchange mechanism, as previously observed for other fast-exchanging monohydrated Gd^{III} poly(aminocarboxylate) complexes.[3b] However, this hypothesis could only be verified by variable pressure ^{17}O NMR experiments.

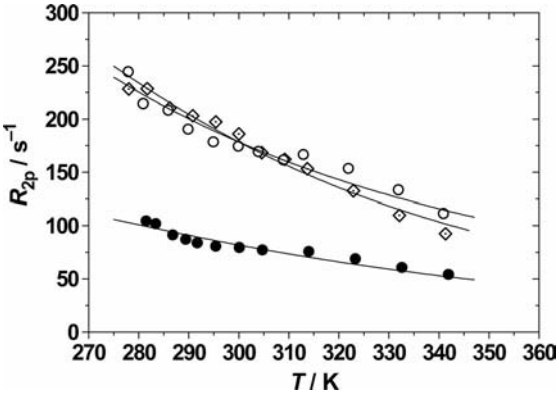

Figure 4. Variation of the transverse ^{17}O relaxation rate, R_{2p}, with temperature for [Gd**L1**]$^-$ (23 mM; diamonds), [Gd**L2**]$^-$ (9 mM; filled circles)[4] and [Gd**L3**]$^-$ (24 mM; open circles)[4] at 2.1 T and pH = 7.

The two complexes bearing a lipophilic pendant chain, [Gd**L4**–**L5**]$^-$, are expected to show the ability to self-assemble into micelles.[15] For [Gd**L5**]$^-$, this is clearly indicated by its relaxivity value (Figure 2), whereas for [Gd**L4**]$^-$, the micelle formation was assessed by measuring the observed relaxation rate (20 MHz, 298 K) as a function of increasing concentration of the complex. In the region above the critical micellar concentration (cmc), the relaxation rate is conveniently expressed as the sum of two contributions, one attributable to the monomeric complex (present in solution at the concentration corresponding to the cmc) and the second assigned to the micellar aggregate. The relaxation rate of the paramagnetic system can then be expressed as in Equation (1), where $r_1^{n.a.}$ and r_1^a are the proton relaxivities of the nonaggregated and aggregated forms, respectively, R_1^d corresponds to the relaxation rate of pure water (0.38 s^{-1} at 20 MHz and 298 K) and C is the analytical concentration of Gd^{III}.

$$R_1^{obs} - R_1^d = (r_1^{n.a.} - r_1^a) \times cmc + r_1^a \times C \quad (1)$$

The relaxivity of the monomeric, isolated complex, $r_1^{n.a.}$, is simply given by Equation (2).

$$R_1^{obs} - R_1^d = r_1^{n.a.} \times C \quad (2)$$

By plotting $R_1^{obs} - R_1^d$ as a function of the parameter C, cmc, $r_1^{n.a.}$ and r_1^a can be obtained by fitting Equations (1) and (2), as shown in Figure 5.[16] The relaxivity of

[Gd**L4**]$^{-}$ assumes the value of 7.6 ± 0.1 mm^{-1} s^{-1} below the cmc, 11.1 ± 0.2 mm^{-1} s^{-1} above the cmc, whereas the cmc is 0.08 ± 0.01 mm. In case of [Gd**L5**]$^{-}$, the cmc value is below 0.05 mM and thus could not be measured by relaxometry.

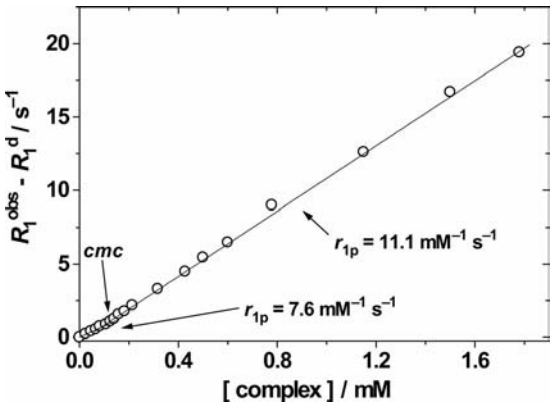

Figure 5. Plot of the water ^{1}H longitudinal relaxation rate at 20 MHz and 298 K as a function the total Gd^{III} concentration for [Gd**L4**]$^{-}$ and the least-squares fit according to Equation (1).

The NMRD profiles of the aggregated form of the complexes exhibit a different amplitude but share a general shape with a broad hump centred around ca. 30 MHz, typical of slowly tumbling systems (Figure 6).[15,17] A different approach is required for the analysis of the profiles, because of the presence of two types of motion characterized by quite diverse correlation times: a relatively fast local rotation of the coordination cage about the main axis of the aliphatic chain superimposed on the global motion of the micelle. A typical and effective approach is based on the incorporation of the description of the rotational dynamics into the Solomon–Bloembergen–Morgan equations for the *inner-sphere* relaxation mechanism according to the model-free Lipari–Szabo approach.[18] This model takes into account both the contribution of the overall global rotation of the paramagnetic micelle (τ_{RG}) and the presence of a faster local motion (τ_{RL}) due to the free rotation of the metal chelate about the pendant arm. The degree of correlation between the two types of motion is given by the parameter S^2 whose value is between zero (completely independent motions) and one (entirely correlated motions). A least-square fit of the data was performed by fixing the values of q, r, τ_M, a, and D and treating the parameters Δ^2, τ_V, τ_{RG}, τ_{RL} and S^2 as variables. For the residence lifetime, τ_M, the value obtained for [Gd**L1**]$^{-}$ was used since it could not be determined by ^{17}O NMR spectroscopy due to the relatively low solubility of the complexes (1–2 mM). The best-fit parameters are listed in Table 2 and clearly show that small differences in the rotational dynamics of the two micellar systems is entirely responsible for their different relaxivity profiles. In fact, [Gd**L4**]$^{-}$ and [Gd**L5**]$^{-}$ show a difference in the correlation times associated with the overall tumbling motion (2.2 and 2.4 ns, respectively) and, even more pronounced, in the order parameter (0.10 and 0.073). Both systems are therefore highly flexible and their relaxivity is mostly modulated by the local rotation. For this reason the parameter τ_{RG} is affected by a large error and is ill defined. The higher relaxivity of [Gd**L4**]$^{-}$ can simply be attributed to the higher S^2 value, which reflects a slightly better correlation between the two types of motion.

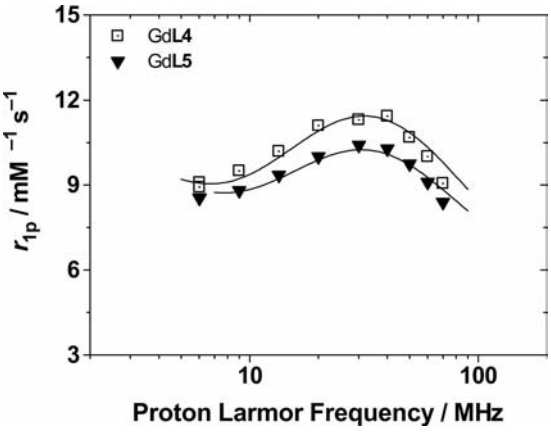

Figure 6. $1/T_1$ ^{1}H NMRD profiles of the aggregated form of [Gd**L4**]$^{-}$ and [Gd**L5**]$^{-}$ at 298 K. The solid lines are calculated with the parameters reported in Table 2.

Table 2. Selected best-fit relaxation parameters obtained from the analysis of the $1/T_1$ NMRD profiles (298 K) of [Gd**L4**]$^{-}$ and [Gd**L5**]$^{-}$.[a]

	r_{1p} [mM^{-1} s^{-1}]	Δ^2 [(10^{19} s^{-2}]	τ_V [ps]	τ_{RG} [ns]	τ_{RL} [ps]	S^2
[Gd**L4**]$^{-}$	11.1	2.0	51	2.2	116	0.10
[Gd**L5**]$^{-}$	10.0	2.1	50	2.4	119	0.073

[a] For the parameters a, ^{298}D, q and r, the values 4.0 Å, 2.24×10^{-5} cm^2 s^{-1}, 1 and 3.0 Å, respectively, were used.

Interaction with HSA

The presence of pendant hydrophobic groups on the Gd^{III} complexes enables noncovalent interaction with hydrophobic binding sites on human serum albumin (HSA).[11,19] The noncovalent binding with plasma proteins is generally exploited for increasing the lifetime of the paramagnetic probe in the vascular system for angiographic MRI applications and is accompanied by a strong enhancement of the relaxivity because of the decreased rate of tumbling (lengthening of τ_R).[20] However, the observed maximum relaxation rate enhancement of the bound Gd^{III} complexes investigated so far is typically much lower than that expected on the basis of theoretical simulations.[8,9,17] This has been explained by the occurrence of slow water exchange rates and/or relatively fast local rotation of the metal complex about the targeting group.[21,22]

The presence of hydrophobic groups allows the [Gd**L2**–**L5**]$^{-}$ complexes to bind HSA with different affinity. Furthermore, whereas all the complexes are characterized by a fast rate of water exchange, they only differ in the length and flexibility of the lipophilic moiety thus enabling

a clear assessment of the limiting effect of local rotation on the relaxivity enhancement of the conjugated complexes. [Gd**L2**]$^-$ represents a model system that incorporates into the ligand backbone a rigid group able to interact with HSA and that is characterized by the presence of one, fast exchanging, bound water molecule. In fact, for this system, a relaxivity value of about 80 $mM^{-1}s^{-1}$ (per Gd ion and per bound water molecule; 30 MHz, 25 °C) is measured, i.e. more than 30% higher than that of any other HSA-bound Gd complex so far reported.[4] This has been attributed to the simultaneous optimization of the rotational dynamics and water exchange rate, thus confirming the validity of the predictions made by the existing theory.[8,9]

The binding interaction has been investigated through the well-established proton relaxation enhancement (PRE) technique that consists of measuring the increase in the water proton longitudinal relaxation rate (R_1) as a function of increasing concentration of the protein at 20 MHz and 298 K (Figure 7).[5,19] R_1 is enhanced by the increase in the fraction of bound complex and the decrease in its reorientational motion in the adduct. The fitting of the experimental data to the theoretical values calculated on the basis of established theory provides the values of the thermodynamic association constant, K_A, the number of the equivalent and independent binding sites, n, and the relaxivity of the resulting paramagnetic metalloprotein, r_1^{bound}.

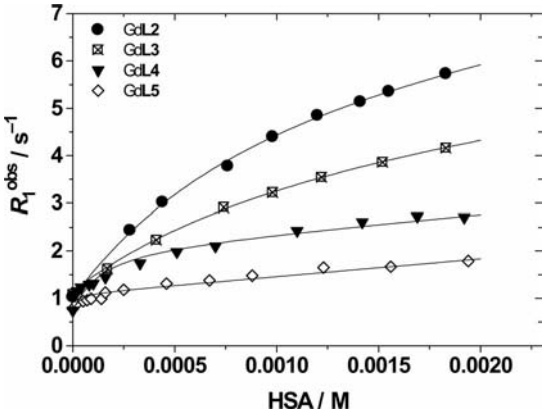

Figure 7. Plot of the water proton longitudinal relaxation rate of a solution of the complexes [Gd**L2**]$^-$ (0.11 mM), [Gd**L3**]$^-$ (0.10 mM), [Gd**L4**]$^-$ (0.05 mM) and [Gd**L5**]$^-$ (0.04 mM) as a function of HSA concentration at 20 MHz, 298 K and pH = 7.0.

All the data were fitted to a 1:1 binding isotherm even though the presence of multiple affinity sites on HSA cannot be excluded for these complexes. The affinity of the complexes for the protein is dictated by the length and flexibility of the pendant hydrophobic moiety: K_A is ca. 1×10^3 M^{-1} for [Gd**L2**,**3**]$^-$ bearing simple naphthalene and benzyl groups and increases by about one and two orders of magnitude for the complexes bearing long C_{12}– ([Gd**L4**]$^-$) and C_{18}– ([Gd**L5**]$^-$) alkyl chains, respectively (Table 3). These values are quite consistent with similar data reported for complexes bearing analogous targeting groups.[23,24] In particular, for [Gd**L5**]$^-$ the binding occurs for concentrations above the critical micellar concentration, as reported for a lipophilic derivative of GdAAZTA bearing a $-C_{17}$ alkyl chain.[24] In that case, the data were interpreted in terms of a supramolecular adduct formed between the preformed micelle and HSA. This type of association is likely to be controlled by electrostatic interactions among the negative charges of the micelles and the positively charged residues exposed on the surface of the protein. The r_{1p}^{bound} values (20 MHz and 298 K) span a rather broad range of values: from 68 $mM^{-1}s^{-1}$ for the highly compact and rigid [Gd**L2**]$^-$ complex to 18 $mM^{-1}s^{-1}$ for the complex [Gd**L5**]$^-$ functionalized with the C_{18}– alkyl chain. By increasing the length of the pendant group the degree of local motions involving the coordination cage increases, which results in a poor motional coupling between the paramagnetic unit and the protein (shorter effective rotational correlation time) and thus in lower relaxivity.

Table 3. Best-fit parameters obtained from the analysis of the relaxometric titrations (20 MHz; 298 K) of [Gd**L2**–**L5**]$^-$ with HSA.

	[Gd**L2**]$^-$	[Gd**L3**]$^-$	[Gd**L4**]$^-$	[Gd**L5**]$^-$
$n \cdot K_A$ [M^{-1}]	880 ± 100	940 ± 90	9716 ± 902	81400 ± 4080
r_{1p}^{bound} [$mM^{-1}s^{-1}$]	68 ± 2	45 ± 3	36 ± 4	18 ± 2
r_{1p}^{free} [$mM^{-1}s^{-1}$]	5.7 ± 0.2	7.0 ± 0.3	7.4	10.0 ± 0.4

Optimization of the rate of water exchange of the Gd chelates does not necessarily lead to significant relaxivity enhancement. The limiting of the local motion of the gadolinium centre must also be considered a fundamental requirement for in the development of highly efficient macromolecular systems.

Docking Results

Gd-based MRI contrast agents bearing a hydrophobic moiety are known to bind to HSA[25] mainly through the two drug binding sites: Sudlow's site I and site II.[26] The different Gd^{III} complexes reported in this study have different binding moieties, both from a chemical and from a size/length point of view. For this reason, the binding modes to HSA are expected to be different for the various complexes. Computational methods based on the calculation of the interaction energies (docking procedure) between the complexes and the protein were utilized to explore possible binding modes and to discriminate between the two main drug binding sites. The modelling results were compared to competitive binding assays, by a relaxometric procedure, with substrates known to tightly bind HSA, e.g. Ibuprofen and Warfarin.[26] These experiments have been performed by titrating a dilute solution of the complex with a solution containing HSA and the specific probe molecule (Warfarin for site I and Ibuprofen or Diclofenac for site II) in the stoichiometric ratio 1:1 and by measuring the change in the relaxation rate. Since the competitor probes bind HSA with affinity constant values more than two orders of magnitude higher than that of the Gd^{III} complexes,[19] their sites should no longer be available to the metal chelates. A decrease in the observed relaxation rates relative to the corresponding data in the absence of the competitor indi-

cates a preferential binding of the complex for the specific site.

[Gd**L2**]$^{-}$ features the shorter and more rigid binding moiety, with the naphthalene group able to penetrate inside the binding cavity both for site I and site II. On the basis of the calculated interaction energies (Table 4), the complex is expected to bind more strongly to site II rather than to site I. This result is in agreement with an experimental competition assay, where [Gd**L2**]$^{-}$ is found to be displaced by a greater extent by Diclofenac (see Supporting Information). The complex [Gd**L3**]$^{-}$ presents a binding moiety completely different from [Gd**L2**]$^{-}$, bearing both hydrophobic and polar groups that allow for different binding modes. The docking results combined with the interaction energy calculations indicate a preference for binding site I. Further, in this case, the docking results are confirmed by relaxometric experiments where a competitive assay with Warfarin indicates that the stronger binding region is represented by site I (see Supporting Information). For the complex [Gd**L4**]$^{-}$, possessing a long hydrophobic chain, the docking results and the calculated interaction energies do not point to a particular affinity towards one of the two binding sites. It could be suggested that the long hydrophobic tail of [Gd**L4**]$^{-}$ penetrates equally well in both sites I and II, with similar interaction energies, because of the lack of specificity of the aliphatic chain with respect to the binding cavity.

Table 4. Calculated interaction energies and experimental competition studies for the two HSA binding sites, I and II.[a]

Ligand	Calculated interaction energy [kcal/mol]		Experimental competition	
	Site I	Site II	Site I	Site II
[Gd**L2**]$^{-}$	–294,81	–565,37	–	Diclofenac
[Gd**L3**]$^{-}$	–479,53	–215,99	Warfarin	–
[Gd**L4**]$^{-}$	–300,40	–134,33	–	–

[a] The binding affinities in Table 3 were used in the calculations.

Conclusions

The "rigidification" of the oxyethylene bridge by incorporation of an aromatic group does not alter the structural properties of the parent complex and allows: (i) to increase the stereochemical rigidity of the metal chelates; (ii) to increase the steric interaction with the inner coordination sphere water molecule thus accelerating its exchange; (iii) to provide the complexes with the presence of remote functional groups that favour the conjugation of the complexes to HSA. The occurrence of a fast rate of water exchange enhances the efficacy of the macromolecular adducts with the protein. Moreover, the degree of relaxivity enhancement is strictly correlated with the reduction of the internal rotation about the targeting hydrophobic group. The simultaneous optimization of the motional coupling between the metal chelate and the large protein and the rate of water exchange yields a relaxivity as high as 80 $mM^{-1} s^{-1}$ ([Gd**L2**]$^{-}$; 30 MHz, 298 K), which is quite close to the maximum predicted by the theoretical simulations.

Experimental Section

General: All chemicals were purchased from Sigma–Aldrich S.R.L. (Milan, Italy) and were used without purification. ESI mass spectra were recorded with a Waters SQD 3100 instrument.

Synthesis of Ln[L1]$^{-}$ Complexes: $Ln(NO_3)_3 \cdot 6H_2O$ (0.05 mmol) was added in small portions to a water solution (0.5 mL, pH = 6) of **L1** (21 mg, 0.05 mmol) with magnetic stirring. After 2 h, the solution was filtered and lyophilized to obtain a white powder.

[LaL1]$^{-}$: ^{1}H NMR (D_2O, 298 K): δ = 6.83 (s, 4 H, 14-H to 17-H), 4.06 (s, 4 H, 10-H, 11-H), 3.18 (m, 8 H, 5-H to 8-H), 2.80 (s, 4 H, 9-H, 12-H) ppm. ^{13}C NMR (D_2O, 298 K): δ = 179.7 (C-1, C-2, C-3,C-4), 145.7 (C-13, C-18), 122.7 (C-15, C-16), 112.9 (C-14, C-17), 67.0 (C-10, C-11), 61.6 (C-5–C-8), 55.5 (C-9, C-12) ppm. MS (ESI^{-}): calcd. for $C_{18}H_{20}LaN_2O_{10}$ [M]$^{-}$: 563.02; found 563.15.

[LuL1]$^{-}$: ^{1}H NMR (D_2O, 298 K): δ = 6.90 (d, 4 H, 14-H to 17-H), 4.42, 4.02 (br. s, 4 H, 10-H, 11-H), 3.35 (m, 8 H, H-5–H-8), 3.15, 2.78 (br. s, 4 H, 9-H, 12-H) ppm. ^{13}C NMR (D_2O, 298 K): δ = 180.2, 180.0 (C-1, C-2, C-3,C-4), 144.7 (C-13, C-18), 123.9 (C-15, C-16), 113.6 (C-14, C-17), 68.1 (C-10, C-11), 63.4, 61.4 (C-5–C-8), 57.2 (C-9, C-12) ppm. MS (ESI^{-}):calcd. for $C_{18}H_{20}LuN_2O_{10}$ [M]$^{-}$: 599.05; found 599.16.

Synthesis of Ln[L2]$^{-}$ Complexes: $Ln(NO_3)_3 \cdot 6H_2O$ (0.05 mmol) was added in small portions to a water solution (0.5 mL, pH = 6) of **L2** (24 mg, 0.05 mmol) with magnetic stirring. After 2 h, the solution was filtered and lyophilized to obtain a white powder.

[LaL2]$^{-}$: ^{1}H NMR (D_2O, 298 K): δ = 7.84 (m, 2 H, 16-H, 19-H), 7.52 (m, 2 H, 17-H, 18-H), 7.43 (s, 2 H, 14-H, 21-H), 4.37 (s, 4 H, 10-H, 11-H), 3.46 (m, 8 H, H-5–H-8), 3.10 (s, 4 H, 9-H, 12-H) ppm. ^{13}C NMR (D_2O, 298 K): δ = 179.9 (C-1, C-2, C-3,C-4), 146.4 (C-13, C-22), 129.5 (C-15, C-20), 127.0, 125.8 (C-16–C-19), 109.0 (C-14, C-21), 67.6 (C-10, C-11), 61.8 (C-5–C-8), 55.9 (C-9, C-12) ppm. MS (ESI^{-}): calcd. for $C_{22}H_{22}LaN_2O_{10}$ [M]$^{-}$: 613.03; found 613.20.

[LuL2]$^{-}$: ^{1}H NMR (D_2O, 278 K): δ = 7.30 (m, 2 H, 16-H, 19-H), 7.21 (m, 2 H, 17-H, 18-H), 6.74 (s, 2 H, 14-H, 21-H), 4.26, 4.01 (s, 4 H, 10-H, 11-H), 3.52 (m, 8 H, H-5–H-8), 3.27, 2.93 (s, 4 H, 9-H, 12-H) ppm. ^{13}C NMR (D_2O, 298 K): δ = 180.5, 180.0 (C-1, C-2, C-3,C-4), 143.9 (C-13, C-22), 129.4 (C-15, C-20), 127.2, 126.2 (C-16–C-19), 109.4 (C-14, C-21), 68.8 (C-10, C-11), 63.0, 62.5 (C-5–C-8), 57.7 (C-9, C-12) ppm. MS (ESI^{-}): calcd. for $C_{22}H_{22}LuN_2O_{10}$ [M]$^{-}$: 649.07; found 649.30.

NMR Experiments: ^{1}H and ^{13}C NMR spectra were recorded at 11.75 T (500 MHz, ^{1}H; 125.7 MHz, ^{13}C) on a Bruker Avance III spectrometer and at 9.7 T (400 MHz) on a JEOL ECP spectrometer. Chemical shifts are reported as δ values. The temperature was controlled with Bruker/JEOL thermostatting units and measured by the chemical shift difference of the methanol resonances. For measurement in D_2O, *tert*-butyl alcohol was used as an internal standard with the methyl signal calibrated at δ = 1.2 (^{1}H) and 30.3 ppm (^{13}C). Spectra assignments are based on COSY and HSQC experiments.

^{1}H and ^{17}O NMR Relaxation Measurements: The water proton longitudinal relaxation rates as a function of the magnetic field strength were measured with a Stelar Spinmaster Spectrometer FFC-2000 (Mede, Pv, Italy) on about 0.5–2.5 mM solutions of [Gd**L1**–**L5**]$^{-}$ complexes in non-deuterated water. The exact concentration of gadolimium was determined by measurement of bulk magnetic suceptibility shifts of a *t*BuOH signal and/or by ICP-OES. The ^{1}H T_1 relaxation times were acquired by the standard inversion recovery method with typical 90° pulse width of 3.5 μs,

16 experiments of 4 scans. The reproducibility of the T_1 data was ±5%. The temperature was controlled with a Stelar VTC-91 airflow heater equipped with a calibrated copper–constantan thermocouple (uncertainty of ±0.1 °C). The proton $1/T_1$ NMRD profiles were measured on a fast field-cycling Stelar SmartTracer relaxometer over a continuum of magnetic field strengths from 0.00024–0.25 T (corresponding to 0.01–10 MHz proton Larmor frequencies). The relaxometer operates under computer control with an absolute uncertainty in $1/T_1$ of ± 1%. Additional data points in the range 15–70 MHz were obtained on a Bruker WP80 NMR electromagnet adapted to variable-field measurements (15–80 MHz proton Larmor frequency) Stelar Relaxometer. Variable-temperature ^{17}O NMR measurements were recorded on a JEOL EX-90 (2.1 T) spectrometer equipped with a 5-mm probe and standard temperature control units. Aqueous solutions of the complexes (10–20 mM) containing 2.0% of the ^{17}O isotope (Cambridge Isotope) were used. The observed transverse relaxation rates were calculated from the signal width at half-height.

Computational Methods: The docking procedure was applied to [Gd**L2**–**L4**]$^-$ complexes with fatted Human Serum Albumin (HSA) by using the MOE molecular modelling package (MOE Version 2004.03 Chemical Computing Group Inc. Montreal, Canada).

The crystal structure of HSA was taken from Brookhaven Protein Databank (PDB code 1e7h www.rcsb.org/pdb) and prepared to docking calculations by adding hydrogen atoms, completing the missing side-chain and minimizing the structures with a multistep procedure.[27,28]

Gd complexes were built from the crystal structure of [Gd(EGTA)]$^-$ obtained from the CSD (entry code FAFGEZ; www.ccdc.cam.ac.uk/).

Structures were energy minimized and atomic charges were calculated on all Gd atoms at the RHF level by the Mulliken method with the program Gamess[29] with a 6-31G** basis set for ligand atoms. Gd atom was treated by using the effective core potential (ECP) of Dolg et al.[30] that includes 4f electrons in the core.

For all the molecular mechanics calculations, a modification of the MMFF94 force field[31] with in-house parameterization to treat the Gd complexes was utilized. Conformational analysis of [Gd**L3**]$^-$ and [Gd**L4**]$^-$ was done with a systematic search on rotatable bonds. Docking procedures were performed with the ligands kept partially flexible by using a Tabu Search method (10 runs, 1000 steps per run) and a random initial orientation. An implicit solvation contribution (continuum model) was included to model solvent effects[32] during the docking calculations. The results of the docking calculations were sorted by utilizing a force-field-based scoring function. For each complex, we chose the five best poses after the docking calculation and compared the interaction energy in the two binding cavities.

Supporting Information (see footnote on the first page of this article): Comments on the NMRD analysis, ^1H and ^{13}C NMR spectra of the La^{III} and Lu^{III} complexes of [**L2**]$^-$, VT ^{13}C NMR spectra of the acetic $-CH_2$ region for [Lu**L2**]$^-$ and plots for the binding of [Gd**L2**]$^-$ and [Gd**L3**]$^-$, alone and in combination with displacer drugs, to HSA.

Acknowledgments

Financial support from the Ministero dell'Istruzione, dell'Università e della Ricerca (MIUR) (PRIN 2007) and the Regione Piemonte (Nano-IGT project) are gratefully acknowledged. This work was carried out under the auspices of Consorzio Interuniversitario di Ricerca in Chimica dei Metalli nei Sistemi Biologici (CIRCMSB) and the European Cooperation in Science and Technology (COST) (Action D38).

[1] L. Tei, Z. Baranyai, M. Botta, L. Piscopo, S. Aime, G. B. Giovenzana, *Org. Biomol. Chem.* **2008**, *6*, 2361.
[2] S. Aime, A. Barge, A. Borel, M. Botta, S. Chemerisov, A. E. Merbach, U. Muller, D. Pubanz, *Inorg. Chem.* **1997**, *36*, 5104.
[3] a) S. Aime, M. Botta, M. Fasano, E. Terreno, *Acc. Chem. Res.* **1999**, *32*, 941–949; b) L. Helm, A. E. Merbach, *Chem. Rev.* **2005**, *105*, 1923–1959.
[4] S. Avedano, L. Tei, A. Lombardi, G. B. Giovenzana, S. Aime, D. Longo, M. Botta, *Chem. Commun.* **2007**, 4726.
[5] a) R. A. Dwek, *Nuclear Magnetic Resonance in Biochemistry Application to Enzyme Systems*, Clarendon Press, Oxford, **1973**, pp. 247–284; b) B. G. Jenkins, E. Armstrong, R. B. Lauffer, *Magn. Reson. Med.* **1991**, *17*, 164; c) A. S. Mildvan, M. Cohen, *Biochemistry* **1963**, *2*, 910–919.
[6] H. Friebolin, *Basic One- and Two-Dimensional NMR Spectroscopy*, 2nd ed.; VCH, Weinheim, Germany, **1993**, pp. 293–296.
[7] R. C. Holz, S. L. Klakamp, C. A. Chang, W. D. Horrocks Jr., *Inorg. Chem.* **1990**, *29*, 2651–2658.
[8] P. Caravan, J. J. Ellison, T. J. McMurry, R. B. Lauffer, *Chem. Rev.* **1999**, *99*, 2293–2352.
[9] a) É. Toth, L. Helm, A. E. Merbach in *The Chemistry of Contrast Agents in Medical Magnetic Resonance Imaging* (Eds.: A. E. Merbach; É. Toth), **2001**, John Wiley & Sons, Chichester, UK, Chapter 2; b) S. Aime, M. Botta, E. Terreno, *Adv. Inorg. Chem.* **2005**, *57*, 173–237.
[10] S. H. Koenig, R. D. Brown III, *Prog. Nucl. Magn. Reson. Spectrosc.* **1990**, *22*, 487–567.
[11] R. B. Lauffer, *Chem. Rev.* **1987**, *87*, 901–927.
[12] S. Aime, M. Botta, M. Fasano, E. Terreno, *Chem. Soc. Rev.* **1997**, *26*, 1–11.
[13] K. Micksei, D. H. Powell, L. Helm, E. Brucher, A. E. Merbach, *Magn. Reson. Chem.* **1993**, *31*, 1011–1020.
[14] T. J. Swift, R. E. Connick, *J. Chem. Phys.* **1962**, *37*, 307.
[15] G. M. Nicolle, É. Tóth, K. P. Eisenwiener, H. R. Mäcke, A. E. Merbach, *J. Biol. Inorg. Chem.* **2002**, *7*, 757.
[16] S. Torres, J. A. Martins, J. P. André, C. F. G. C. Geraldes, A. E. Merbach, E. Toth, *Chem. Eur. J.* **2006**, *12*, 940.
[17] D. Delli Castelli, E. Gianolio, S. Geninatti Crich, E. Terreno, S. Aime, *Coord. Chem. Rev.* **2008**, *252*, 2424–2443.
[18] a) G. Lipari, S. Szabo, *J. Am. Chem. Soc.* **1982**, *104*, 4546; b) G. Lipari, S. Szabo, *J. Am. Chem. Soc.* **1982**, *104*, 4559.
[19] a) S. Aime, M. Botta, M. Fasano, E. Terreno in *The Chemistry of Contrast Agents in Medical Magnetic Resonance Imaging* (Eds.: A. E. Merbach; É. Toth), **2001**, John Wiley & Sons, Chichester, UK, ch. 5; b) S. Aime, M. Botta, M. Fasano, S. Geninatti Crich, E. Terreno, *J. Biol. Inorg. Chem.* **1996**, *1*, 312–319.
[20] P. Caravan, *Acc. Chem. Res.* **2009**, *42*, 851–862.
[21] Z. Zhang, M. T. Greenfield, M. Spiller, T. J. McMurry, R. B. Lauffer, P. Caravan, *Angew. Chem.* **2005**, *117*, 6924; *Angew. Chem. Int. Ed.* **2005**, *44*, 6766–6769.
[22] F. Kielar, L. Tei, E. Terreno, M. Botta, *J. Am. Chem. Soc.* **2010**, *132*, 7836–7837.
[23] P. Caravan, M. T. Greenfield, X. Li, A. D. Sherry, *Inorg. Chem.* **2001**, *40*, 6580.
[24] E. Gianolio, G. B. Giovenzana, D. Longo, I. Longo, I. Menegotto, S. Aime, *Chem. Eur. J.* **2007**, *13*, 5785.
[25] G. Sudlow, D. J. Birkett, D. N. Wade, *Mol. Pharmacol.* **1975**, *11*, 824.
[26] X. M. He, D. C. Carter, *Nature* **1992**, *358*, 209.
[27] G. Ermondi, G. Caron, G. M. Lorenti, *J. Med. Chem.* **2004**, *47*, 3949.
[28] I. T. Christensen, F. S. Jorgensen, *J. Biomol. Struct. Dyn.* **1997**, *15*, 473.

[29] M. W. Schmidt, K. K. Baldridge, J. A. Boatz, S. T. Elbert, M. S. Gordon, J. H. Jensen, S. Koseki, N. Matsunaga, K. A. Nguyen, S. Su, T. L. Windus, M. Dupuis, J. A. Montgomery, *J. Comput. Chem.* **1993**, *14*, 1347.
[30] M. Dolg, H. Stoll, A. Savin, H. Preuss, *Theor. Chim. Acta* **1989**, *75*, 173.
[31] T. A. Halgren, *J. Comput. Chem.* **1996**, *17*, 490.
[32] D. Qiu, P. S. Shenkin, F. P. Hollinger, W. C. Still, *J. Phys. Chem.* **1997**, *101*, 3005.

Received: October 15, 2010
Published Online: January 13, 2011

